cases, result in longer taxon ranges than high origination rates (*25*). The paucity of seep taxon origination in the Neogene could indeed reflect low origination rates in the seep environment and thus account (to some extent) for the older-than-average age of seep mollusks. However, deep-sea mollusks show high origination rates in the Neogene, despite their older-than-average age, and considering the lack of effect of the end-Cretaceous extinction event and the anoxic/dysoxic events on both deep-sea and seep taxa, we conclude that paleoenvironmental factors have mainly shaped the age distribution of the modern seep mollusks.

Vents and seeps have been considered extinction-resistant habitats (*3*, *4*). Extinction and survival patterns across the Paleocene/Eocene thermal maximum show a paradox. Planktonic foraminifera and calcareous nannofossils remained abundant, but a significant number of benthic foraminifera became extinct, suggesting a cause that preferentially affected the deep-sea biota (*26*). However, there was no extinction among the seep fauna, deep-sea echinoids (*27*), and higher-level taxa among vent organisms (*28*). Because seep taxa are a mixture of endemics and deep-sea generalists, more work is needed to disentangle whether their apparent resistance to extinction is a seep-related phenomenon or a trait shared with deep sea organisms in general.

### References and Notes


1. L. A. Levin, *Oceanogr. Mar. Biol.* **43**, 1 (2005).
2. C. L. Van Dover, C. R. German, K. G. Speer, L. M. Parson, R. C. Vrijenhoek, *Science* **295**, 1253 (2002).
3. V. Tunnicliffe, *Palaios* **7**, 338 (1992).
4. A. G. McArthur, V. Tunnicliffe, in *Modern Ocean Floor Processes and the Geological Record*, R. A. Mills, K. Harrison, Eds. (Geological Society, London, 1998), vol. 148, pp. 271–291.
5. C. S. Hickman, *Zool. Scr.* **13**, 19 (1984).
6. W. A. Newman, *Bull. Biol. Soc. Wash.* **6**, 231 (1985).
7. D. L. Geiger, C. E. Thacker, *Moll. Res.* **25**, 47 (2005).
8. A. S. Peek, R. G. Gustafson, R. A. Lutz, R. C. Vrijenhoek, *Mar. Biol.* **130**, 151 (1997).
9. K. M. Halanych, R. A. Lutz, R. C. Vrijenhoek, *Cah. Biol. Mar.* **39**, 355 (1998).
10. P. Chevaldonne, D. Jollivet, D. Desbruyères, R. A. Lutz, R. C. Vrijenhoek, *Cah. Biol. Mar.* **43**, 367 (2002).
11. W. J. Jones *et al.*, *Mar. Biol.* **148**, 841 (2006).
12. D. K. Jacobs, D. R. Lindberg, *Proc. Natl. Acad. Sci. U.S.A.* **95**, 9396 (1998).
13. Materials and methods are available as supporting material on *Science* Online.
14. E. N. Powell, W. R. Callender, R. J. J. Stanton, *Palaeogeogr. Palaeoclimatol. Palaeoecol.* **144**, 85 (1998).
15. J. J. Sepkoski, *Bull. Am. Paleontol.* **363**, 1 (2002).
16. S. E. Peters, M. Foote, *Paleobiology* **27**, 583 (2001).
17. J. S. Crampton *et al.*, *Science* **301**, 358 (2003).
18. A. R. Baco, C. R. Smith, A. S. Peek, G. K. Roderick, R. C. Vrijenhoek, *Mar. Ecol. Prog. Ser.* **182**, 137 (1999).
19. C. R. Smith, A. R. Baco, *Oceanogr. Mar. Biol.* **41**, 311 (2003).
20. M. D. Uhen, in *Encyclopedia of Marine Mammals*, W. F. Perrin, B. Würsig, J. G. M. Thewissen, Eds. (Plenum, New York, 2001), pp. 78–81.
21. R. E. Fordyce, C. de Muizon, in *Secondary Adaptation of Tetrapods to Life in Water*, J.-M. Mazin, V. de Buffrénil, Eds. (Dr. Friedrich Pfeil, München, 2001), pp. 169–233.
22. R. L. Squires, J. L. Goedert, L. G. Barnes, *Nature* **349**, 574 (1991).
23. D. Jablonski, J. J. Sepkoski, D. J. Bottjer, P. M. Sheenan, *Science* **222**, 1123 (1983).
24. D. Jablonski, D. J. Bottjer, *Science* **252**, 1831 (1991).
25. M. Foote, in *Evolutionary Patterns*, J. B. C. Jackson, S. Lidgard, F. McKinney, Eds. (Univ. of Chicago Press, Chicago, 2001), pp. 245–294.
26. F. Nunes, R. D. Norris, *Nature* **439**, 60 (2006).
27. A. B. Smith, B. Stockley, *Proc. R. Soc. London Ser. B* **272**, 865 (2005).
28. C. T. S. Little, R. C. Vrijenhoek, *Trends Ecol. Evol.* **18**, 582 (2003).


29. We thank B. Huber, G. Hunt, D. Jablonski, C. Taylor, P. Wignall, J. Young, and three reviewers for their input. S.K. was supported by the Walcott fellowship (Smithsonian Institution) and by a European Union Marie-Curie fellowship.


### Supporting Online Material

www.sciencemag.org/cgi/content/full/313/5792/1429/DC1
SOM Text
References

15 February 2006; accepted 29 June 2006
10.1126/science.1126286

# Temporal and Spatial Enumeration Processes in the Primate Parietal Cortex

**Andreas Nieder,* Ilka Diester, Oana Tudusciuc**

**Humans and animals can nonverbally enumerate visual items across time in a sequence or rapidly estimate the set size of spatial dot patterns at a single glance. We found that temporal and spatial enumeration processes engaged different populations of neurons in the intraparietal sulcus of behaving monkeys. Once the enumeration process was completed, however, another neuronal population represented the cardinality of a set irrespective of whether it had been cued in a spatial layout or across time. These data suggest distinct neural processing stages for different numerical formats, but also a final convergence of the segregated information to form most abstract quantity representations.**

Humans and animals share an evolutionarily ancient quantification system that allows them to approximately estimate the size of a set (its numerosity) without verbal symbols (*1*–*4*). How numerical information can be extracted depends on the presentation format: whether the elements of a set are perceived simultaneously or sequentially. When presented simultaneously as in multiple-item patterns, numerosity can be estimated from a spatial arrangement at a single glance. Here, parallel processing mechanisms are engaged, as indicated by constant reaction times (*5*–*7*), equal numbers of scanning eye movements (*7*), and comparable neural response latencies (*8*) across absolute set size. In contrast, when the elements of a set are presented one by one, they need to be enumerated successively across time (*9*–*11*). This latter process constitutes a nonverbal precursor of real counting, which is a sequential enumeration process via number symbols.

Both human (*12*–*21*) and monkey (*22*, *23*) studies relate the processing of numerical quantity information to the posterior parietal cortex, including the intraparietal sulcus (IPS). However, none of these studies addresses the actual "counting" aspect, namely the abstract accumulation of sensory events one by one. Moreover, it remains unknown whether and how numerical information extracted from temporally and spatially arranged presentations is combined at the neuronal level.

To investigate the role of individual IPS neurons in representing simultaneously and sequentially presented visual quantity, we trained monkeys to discriminate small numerosities. The monkeys had to judge whether two successive task periods (first sample, then test) separated by a 1-s delay contained the same number of items (one to four) (Fig. 1, A and B). If so, the animals had to release a lever. In the sample period, the numerosity was presented randomly: either by multiple-dot patterns showing the number of items simultaneously (the simultaneous protocol, Fig. 1B) or by single dots appearing one by one to indicate the number of items in sequence (the sequential protocol, Fig. 1A) (*24*). We ensured that non-numerical parameters (visuospatial cues in multiple-dot patterns and temporal cues in the sequential presentation protocol) could not be used by the monkeys to solve the task. Controls in the simultaneous protocol included displays in which the circumference (and with it total area), density, and configuration (shapelike or linear) were controlled across different quantities. Controls in the sequential protocol eliminated temporal factors that may covary with increasing numbers of sequential items, such as the total duration of the sample period, the duration of individual items and pauses in between, the total visual energy (or total area across time, respectively), and the regularity (rhythm) of the item sequence (see Table 1 and fig. S1 for details). In the test period, numerosity was always cued by multiple-item displays.

Primate NeuroCognition Laboratory, Hertie-Institute for Clinical Brain Research, Department of Cognitive Neurology, University of Tübingen, Otfried-Müller-Strasse 27, 72076 Tübingen, Germany.

*To whom correspondence should be addressed. E-mail: andreas.nieder@uni-tuebingen.de

The monkeys were first trained on the simultaneous task alone and subsequently on the sequential numerosity discrimination. Initially, they only learned to discriminate sequential numerosity 2 from 4 (and vice versa). To investigate whether the monkeys would understand the concept of sequential numerosity without further training, we introduced transfer tests requiring the monkey to discriminate sequential numerosity 3 from 2 and 4 (see SOM for details). Because the animals were randomly rewarded for their responses in transfer tests, any learning of the "correct" response was impossible. Both monkeys immediately discriminated sequential numerosity 3, with a precision comparable to the baseline discrimination of 2 versus 4 (as indicated by the fact that the slopes for the match and nonmatch discrimination in the transfer and baseline tests are almost parallel) (Fig. 1, C and D). The numerical distance between match and nonmatch in the transfer tests is only one, which is more difficult to discriminate than the baseline discrimination with a numerical distance of two (*25*).

After these transfer tests, monkeys had to perform both the simultaneous and the sequential task within a single session. The average performance of the two monkeys on both the sequential and simultaneous protocols was between 71 and 99% correct (Fig. 1E) and significantly better than chance for all tested quantities (binomial test, $P < 0.001$; see fig. S2 for detailed performance curves). Discrimination of the quantity of sequentially presented items was more difficult for both monkeys (binomial test, $P < 0.01$). The monkeys readily generalized to the control stimulus sets; performance was very similar across them in the sequential and simultaneous protocols (Fig. 1E and fig. S2).

We recorded from 228 randomly selected neurons in the depth of the IPS (Fig. 2, A and B) of two monkeys performing the numerosity discrimination task. Random presentation of either the sequential or simultaneous protocol from trial to trial allowed us to investigate an individual neuron's responses to both presentation types in an unbiased way. A proportion of the tested neurons [27 out of 228 (27/228) or 12%, two-way analysis of variance (ANOVA), with factors (stimulus protocol) × (sample numerosity), $P < 0.01$] showed activity that varied significantly with the number of items during sample presentation in the simultaneous protocol, irrespective of the displays' visuospatial properties (*23*). Even more neurons (58/228 or 25%, two-factor ANOVA, $P < 0.01$) showed maximum discharge in response to a certain number of dots in the sequential protocol. To further test whether the neurons' discharges to the preferred sequential item were unaffected by temporal parameters, we computed a multiple regression analysis with the spike rate to the preferred sequential item as a dependent variable and the duration of the preferred item in a sequence, the duration of the pause preceding the preferred item, and the duration of the previous-to-preferred item as independent variables (*24*). Only 8 of the 58 sequential numerosity-selective neurons exhibited a significant correlation ($P < 0.01$) with temporal parameters and were thus excluded from the pool of numerosity-selective neurons (fig.

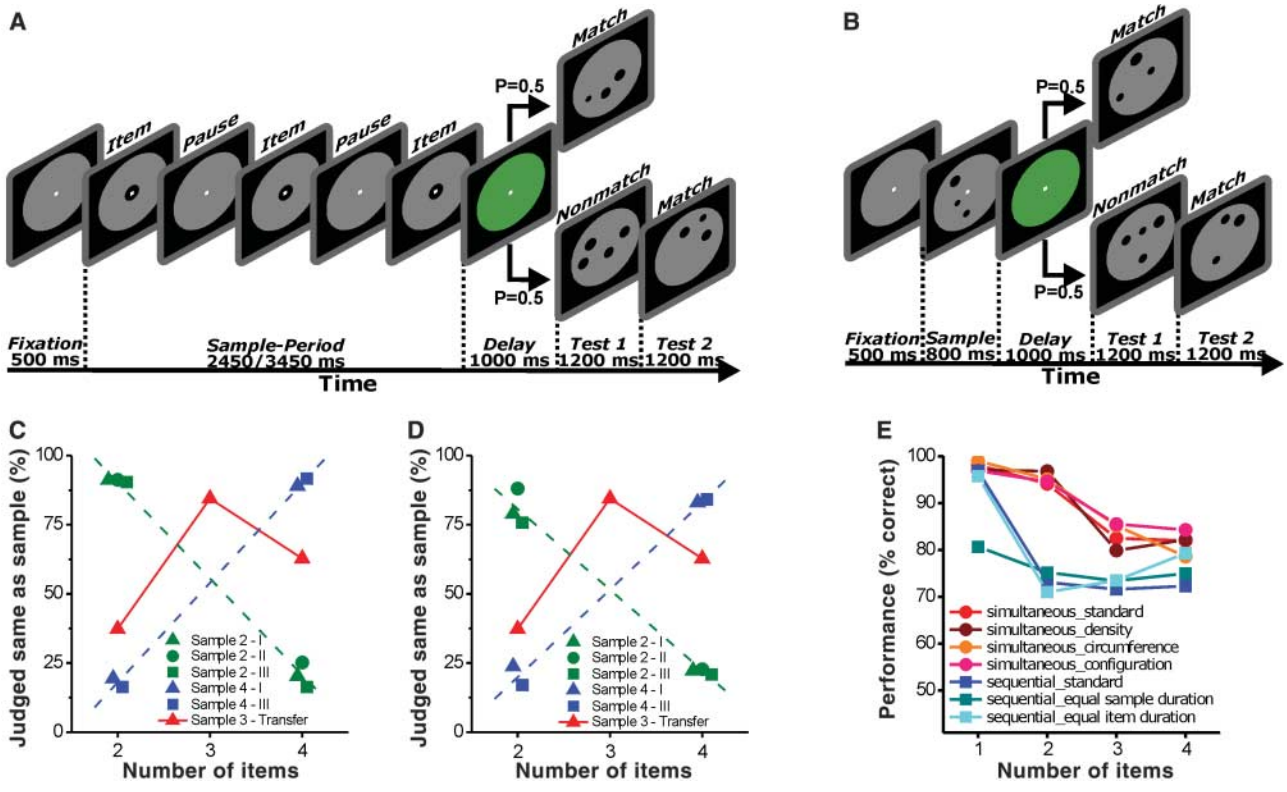


**Fig. 1.** Task protocols and behavioral performance. (**A**) Sequential delayed match-to-quantity task (for example, numerosity 3). A trial started when the monkey grasped a lever. The monkey had to release the lever if the sample period and test display contained the same number of items but continue holding it if they did not (probability of match/nonmatch condition = 0.5). The sample numerosity was cued by sequentially presented items temporally separated by pauses containing no items. The temporal succession and duration of individual items were varied within and across quantities (Table 1). The numerosity in the test period was always cued by multiple-item displays. (**B**) Simultaneous delayed match-to-quantity task. Task conditions were identical to those in the sequential protocol, but numerosity was cued by a single multiple-dot display in the sample period. The physical appearance of the displays varied widely for the same quantities (Table 1). For both the simultaneous and sequential task protocols, the nonmatch stimuli for sample numerosity 1 was 2; for sample 2 the nonmatch numerosities were 1 and 3 (probability = 0.25); for sample numerosity 3 and 4, nonmatches were one and two numbers up and down. (**C** and **D**) Behavioral performance of both monkeys during transfer tests in the sequential task. The monkeys performed a baseline discrimination of 2 versus 4 [green data for different stimulus protocols (I to III) are displayed as listed in Table 1] and 4 versus 2 (blue). Both monkeys [(C) and (D)] spontaneously discriminated sequential numerosity 3 from 2 and 4 in transfer tests without reinforcement (red). (**E**) Average performance of both monkeys in the simultaneous and sequential tasks (under standard and control conditions) during the recording sessions. Chance performance = 50% (also see fig. S2 for details).

S4). Based on the combined results from the two-factor ANOVA and the multiple regression analysis, 50 neurons (from a total of 228 cells; that is, 22%) were found to be selective to sequential quantity only. Two example neurons tuned to sequential numerosity are shown in Fig. 2. The tuning function of the neuron in Fig. 2, C to E, showed peak activity for the sequential quantity 2 and a systematic dropoff of activity as the number of items in the sample period varied from the preferred value (Fig. 2D); this was true even in trials with three or four consecutive dots and varied sequence timing (Fig. 2E). A neuron with preferred numerosity 4 is plotted in Fig. 2, F to H.

Similar response profiles were observed for all neurons tuned to numerosities 1, 2, 3, or 4 in the sequential (see population tuning curves in Fig. 3A) or simultaneous (Fig. 3B) protocol. Each cell showed peak activity for one of the visual quantities and a systematic dropoff of activity as the number of sample items varied from the preferred value (Fig. 3C). Numerosity 1 was the most frequent preferred numerosity in both protocols (Fig. 3D).

Many of the tested neurons (43/228 or 19%) also showed activity that varied significantly during the pauses between item presentation in the sequential protocol (Fig. 1A), irrespective of the temporal arrangement [again tested with a combination of a two-factor ANOVA and a multiple linear regression analysis; see supporting online material (SOM) and fig. S5 for details]. More than half of the neurons that were significantly tuned during the pauses were also tuned during sequential item presentation (25/228 or 11%); thus, the firing rates during item presentations as well as during the pauses between them varied with the position in the sequence. The neuron in Fig. 2F, for example, exhibits a significant increase in discharge during successive pauses, with the highest discharge during the third pause in the sequence. At the same time, this neuron has the preferred item position "four" (Fig. 2, G and H). We found a significant correlation between the neurons' preferred serial position during the pauses and the preferred number of sequential items ($r = 0.70$, $P < 0.001$, $n = 25$ neurons), indicating that the activation of neurons between items could provide a neuronal storage mechanism to keep track of the actual items to enumerate. Such an accumulation of activation was successfully implemented in neural networks simulating numerosity detection (*26*).

A comparison of neurons tuned to numerosity during the sample period in the sequential and simultaneous protocols showed a clear dissociation of neuronal populations. Only 10 neurons (4% of the total sample) were significantly tuned to numerosity in both protocols. Of those 10 cells, only 2 (1% of the total sample) were tuned to the identical numerosity in both the sequential and simultaneous protocols (see neuron in Fig. 2F and fig. S3), which corresponds to chance occurrence. This finding suggests that different populations of neurons are engaged in extracting numerosity in a parallel or serial fashion, respectively (Fig. 3E).

Only after the enumeration process in the sample period was completed did the animals have full information about the cardinality of a set. They had to maintain the quantity in mind throughout a delay period and prepare to find the matching quantity in a test display. Many neurons (43/228 or 19%) were significantly tuned to numerosity only in the memory period, irrespective of the presentation protocol (only significant numerosity effect, two-factor ANOVA with numerosity and presentation protocols as factors, $P < 0.01$). For example, the neuron displayed in Fig. 4 showed remarkably similar delay activity in the sequential (Fig. 4A) and simultaneous (Fig. 4B) presentation protocol, with 3 as the preferred numerosity (Fig. 4C). The average response profiles of all numerosity-selective neurons during the delay period are shown in Fig. 4D. Few cells (9/228 or 4%) were tuned to numerical quantity but also differentiated between the simultaneous and sequential presentations (numerosity and presentation protocol effect or interaction, two-factor ANOVA, $P < 0.01$). Some neurons tuned to the set size in the delay period represented quantity in the sample period (simultaneous protocol: 7/43 or 16%; sequential protocol: 9/43 or 21%).

An examination of error trials suggested that the delay activity of IPS neurons was directly related to the monkeys' performance. When monkeys made judgment errors, neural delay activity for the preferred numerosity was significantly reduced to 83.6% of that observed on correct trials (i.e., 100%) ($P = 0.01$, Wilcoxon signed ranks test, two-tailed).

These results argue for segregated processing of simultaneous and sequential numerical quantity. Different populations of neurons were involved in extracting numerosity across spatial or temporal arrangements during an ongoing quantification process. In contrast, the final and common result of the quantification process was coded by a third population of neurons, irrespective of whether numerosity was cued simultaneously or in sequence. Thus, the intermediate numerosity of an ongoing quantification process and the storage of the final cardinality are accomplished by different neuronal populations.

In contrast to a direct, perceptual-like assessment of numerical information in multiple-item displays, sequential enumeration requires a more complex coding of numerical information. Our data point toward the pauses between individual successive items as a potential key mechanism for the coding of sequential numerosity. For many neurons, activation changes during the pauses were sometimes more prominent than during the presentation of successive items (Fig. 2F). In these neurons, activation to the item presentation seemed to ride on ever-increasing discharges during the pauses, which is consistent with the idea of an accumulator mechanism (*9*, *26*).

The enumeration of sequentially presented items requires an organism to keep track of the serial position of the previously presented item. Similar to our findings in nonhuman primates, neuropsychological (*27*) and electrophysiological

**Table 1.** Stimulus presentation protocols and variation of non-numerical parameters with quantity (w.q.). The timing of the sample period in the sequential protocol was as follows: Standard protocol: sample period duration for all numerosities, 2450 ms; single item/pause duration for numerosity 1, 409 to 1328 ms; numerosity 2, 372 to 1359 ms; numerosity 3, 229 to 1066 ms; numerosity 4, 212 to 607 ms. Equal sample duration protocol: sample period duration for all numerosities, 2450 ms; single item/pause duration for numerosity 1, 2450 ms; numerosity 2, 816 ms; numerosity 3, 490 ms; numerosity 4, 350 ms. Equal item/pause duration protocol: single item/pause duration for all numerosities, 350 ms; sample period duration for numerosity 1, 350 ms; numerosity 2, 1050 ms; numerosity 3, 1750 ms; numerosity 4, 2450 ms. For trials with a sample period duration of 3450 ms, values were correspondingly adjusted.

**Simultaneous protocol**

| Stimulus type | Spatial layout | Surface area | Circumference | Density |
|---|---|---|---|---|
| Standard | Randomized† | Increasing w.q. | Increasing w.q. | Increasing w.q. |
| Circumference | Randomized† | Decreasing w.q. | Equal | Increasing w.q. |
| Density* | Randomized† | Increasing w.q. | Increasing w.q. | Equal |
| Configuration | Linear | Increasing w.q. | Increasing w.q. | Increasing w.q. |

**Sequential protocol**

| Stimulus type | Sample period duration | Individual item or pause duration | Regularity (rhythm) | Intensity over time |
|---|---|---|---|---|
| Standard | Constant | Decreasing w.q. | Irregular | Variable |
| Equal sample duration | Constant | Decreasing w.q. | Regular | Decreasing w.q. |
| Equal item/pause duration | Increasing w.q. | Constant | Regular | Increasing w.q. |

*Density was determined by calculating the average distance between the dots. †High probability that three dots were arranged as a triangle, four dots as a quadrangle, and five dots as pentagon.

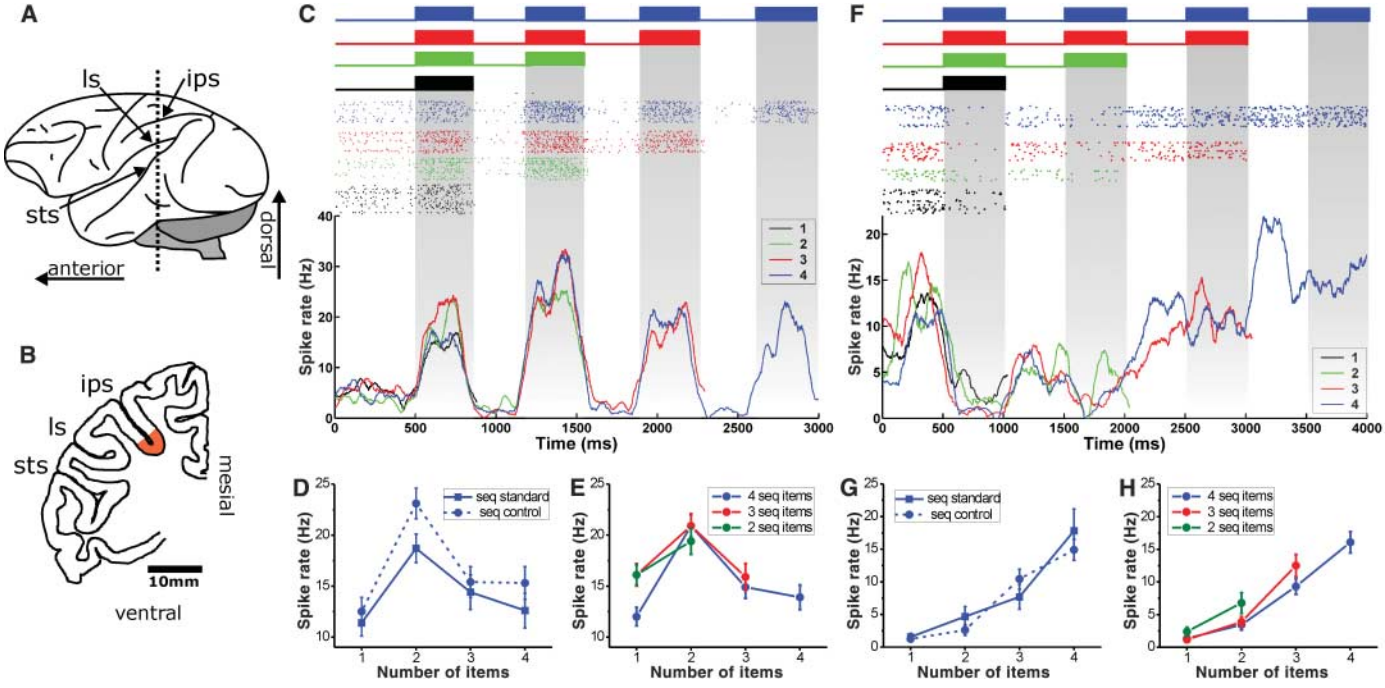


**Fig. 2.** Recording sites and neural responses during sample presentation. (**A**) Lateral view of the left hemisphere of a monkey brain indicating the topographical relationships of cortical landmarks. ips, intraparietal sulcus; ls, lateral sulcus; sts, superior temporal sulcus. (**B**) Coronal section at the level of the dotted line in (A) reconstructed from a structural magnetic resonance imaging scan (Horsley-Clark coordinates 0 mm anterior/posterior). The colored area in the depth of the IPS marks the recording area. (**C** to **E**) Responses of an example neuron selective to the sequential quantity 2 (only the "equal item/pause duration" protocol is shown for clarity). The top panel illustrates the temporal succession of individual items (square pulses represent single items). The corresponding latency-corrected discharges for many repetitions of the protocol are plotted as dot-raster histograms (middle panels; each dot represents an action potential) and averaged spike-density functions (bottom panels; activity averaged and smoothed). The first 500 ms represent the fixation period. Colors correspond for the stimulation illustration and the plotting of the neural data. Gray shaded areas represent item presentation. (D) Rate functions indicate the mean activity of the neuron in (C) to the standard and equal item/pause duration protocols [error bars in (D), (E), (G), and (H) represent the standard error of the mean] for four sequential dots. In both protocols, the neuron was tuned to numerosity 2. (Responses to the first item in a sequence of one, two, three, or four items were not statistically different.) (E) The same neuron shown in (C) was significantly tuned to numerosity 2 irrespective of whether the sample period showed two, three, or four sequential items (standard and control protocols pooled). (**F** to **H**) Neuron tuned to sequential numerosity 4. (F) Neuronal responses for the control protocol [layout as in (C)]. (G) Rate functions show monotonic increase of discharges up to numerosity 4 for both protocols. (H) Comparable discharges of this neuron to the sequential items, irrespective of whether the items were presented in sequences of two, three, or four items.

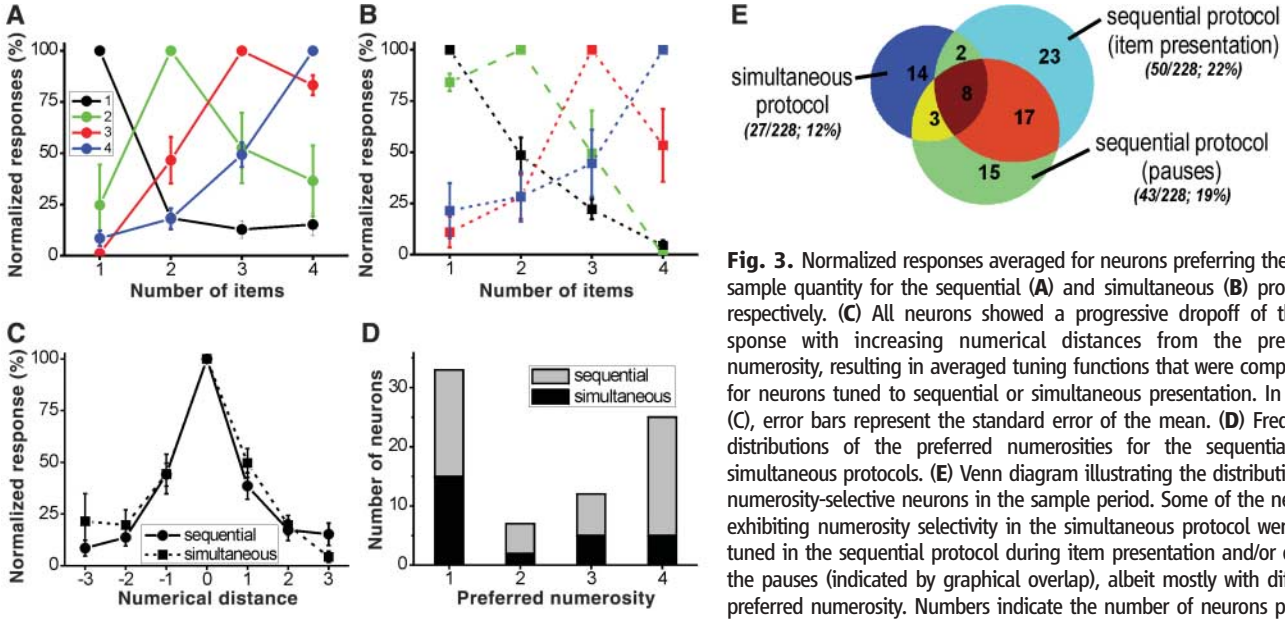


**Fig. 3.** Normalized responses averaged for neurons preferring the same sample quantity for the sequential (**A**) and simultaneous (**B**) protocols, respectively. (**C**) All neurons showed a progressive dropoff of the response with increasing numerical distances from the preferred numerosity, resulting in averaged tuning functions that were comparable for neurons tuned to sequential or simultaneous presentation. In (A) to (C), error bars represent the standard error of the mean. (**D**) Frequency distributions of the preferred numerosities for the sequential and simultaneous protocols. (**E**) Venn diagram illustrating the distributions of numerosity-selective neurons in the sample period. Some of the neurons exhibiting numerosity selectivity in the simultaneous protocol were also tuned in the sequential protocol during item presentation and/or during the pauses (indicated by graphical overlap), albeit mostly with different preferred numerosity. Numbers indicate the number of neurons per set.

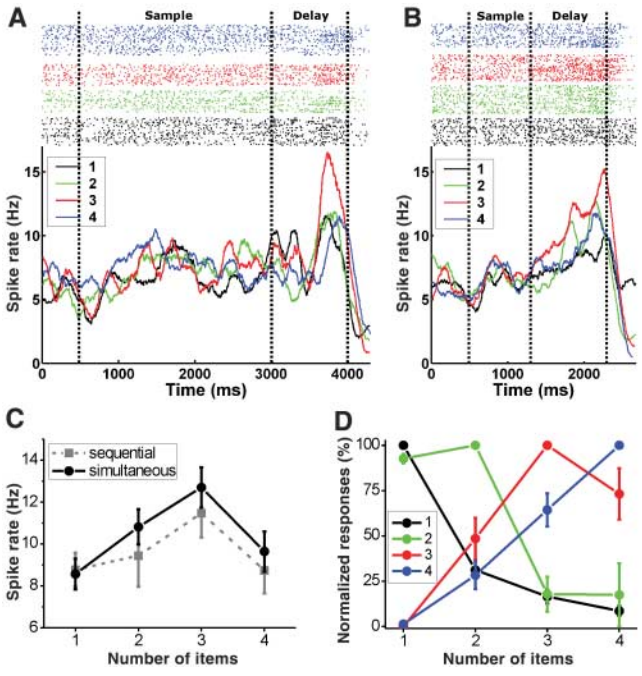


**Fig. 4.** Neural responses during the delay period. (**A** to **C**) A single neuron showing remarkably similar delay activity in the sequential (A) versus simultaneous (B) presentation protocol, with 3 as the preferred numerosity. Top panels in (A) and (B) show color-coded dot-raster histograms; bottom panels are the corresponding spike-density histograms. The first 500 ms represent the fixation period. This neuron was not numerosity-selective in the sample period. (C) Tuning function of the displayed neuron based on averaged discharge rates calculated over the delay period. (**D**) Normalized responses averaged for all neurons preferring the same quantity in the delay period, irrespective of the presentation protocol (sequential and simultaneous). In (C) and (D), error bars represent the standard error of the mean.

(*28*) studies in humans suggest dissociated processes involved in judging cardinality (numerical quantity) as opposed to ordinality (serial position), but sometimes with a common activation in the parietal and prefrontal cortices (*14*, *28*). Neurons in the lateral prefrontal cortex of the monkey are also selectively tuned to numerical rank (*29*) and numerical quantity (*8*), but typically later than IPS neurons (*23*). This suggests that neurons in the posterior parietal and prefrontal cortices are linked to form a single functional network for the representation of numerical information across space and time.

### References and Notes


1. P. Gordon, *Science* **306**, 496 (2004).
2. P. Pica, C. Lemer, V. Izard, S. Dehaene, *Science* **306**, 499 (2004).
3. M. D. Hauser, E. S. Spelke, in *The Cognitive Neurosciences III*, M. Gazzaniga, Ed. (MIT Press, Cambridge, 2004).
4. A. Nieder, *Nat. Rev. Neurosci.* **6**, 177 (2005).
5. H. Barth, N. Kanwisher, E. Spelke, *Cognition* **86**, 201 (2003).
6. J. N. Wood, E. S. Spelke, *Cognition* **97**, 23 (2005).
7. A. Nieder, E. K. Miller, *J. Cogn. Neurosci.* **16**, 889 (2004).
8. A. Nieder, D. J. Freedman, E. K. Miller, *Science* **297**, 1708 (2002).
9. W. H. Meck, R. M. Church, *J. Exp. Psychol. Anim. Behav. Proc.* **9**, 320 (1983).
10. J. Whalen, C. R. Gallistel, R. Gelman, *Psychol. Sci.* **10**, 130 (1999).
11. S. Cordes, R. Gelman, C. R. Gallistel, J. Whalen, *Psychonom. Bull. Rev.* **8**, 698 (2001).
12. L. Cipolotti, B. Butterworth, G. Denes, *Brain* **114**, 2619 (1991).
13. S. Dehaene, L. Cohen, *Cortex* **33**, 219 (1997).
14. S. Dehaene, E. Spelke, P. Pinel, R. Stanescu, S. Tsivkin, *Science* **284**, 970 (1999).
15. E. B. Isaacs, C. J. Edmonds, A. Lucas, D. G. Gadian, *Brain* **124**, 1701 (2001).
16. O. Simon, J. F. Mangin, L. Cohen, D. Le Bihan, S. Dehaene, *Neuron* **33**, 475 (2002).
17. E. Eger, P. Sterzer, M. O. Russ, A. L. Giraud, A. Kleinschmidt, *Neuron* **37**, 719 (2003).
18. P. Pinel, M. Piazza, D. Le Bihan, S. Dehaene, *Neuron* **41**, 983 (2004).
19. M. Piazza, V. Izard, P. Pinel, D. Le Bihan, S. Dehaene, *Neuron* **44**, 547 (2004).
20. D. Ansari, B. Dhita, S. C. Siong, *Brain Res.*, in press.
21. J. F. Cantlon, E. M. Brannon, E. J. Carter, K. A. Pelphrey, *PLoS Biol.* **4**, 844 (2006).
22. H. Sawamura, K. Shima, J. Tanji, *Nature* **415**, 918 (2002).
23. A. Nieder, E. K. Miller, *Proc. Natl. Acad. Sci. U.S.A.* **101**, 7457 (2004).
24. Methods are available as supporting material on *Science* Online.
25. A. Nieder, E. K. Miller, *Neuron* **37**, 149 (2003).
26. S. Dehaene, J. P. Changeux, *J. Cogn. Neurosci.* **5**, 390 (1993).
27. M. Delazer, B. Butterworth, *Cogn. Neuropsychol.* **14**, 613 (1997).
28. E. Turconi, B. Jemel, B. Rossion, X. Seron, *Brain Res. Cogn. Brain Res.* **21**, 22 (2004).
29. Y. Ninokura, H. Mushiake, J. Tanji, *J. Neurophysiol.* **91**, 555 (2004).


30. Supported by a junior research group grant (SFB 550/C11) from the German Research Foundation and a Career Development Award by the International Human Frontier Science Program Organization to A.N. This paper is dedicated to Bärbel.


### Supporting Online Material

www.sciencemag.org/cgi/content/full/313/5792/1431/DC1
Methods
Figs. S1 to S7
References

22 May 2006; accepted 20 July 2006
10.1126/science.1130308

# Isolated Chloroplast Division Machinery Can Actively Constrict After Stretching

**Yamato Yoshida,[1]* Haruko Kuroiwa,[1] Osami Misumi,[1] Keiji Nishida,[1] Fumi Yagisawa,[1] Takayuki Fujiwara,[1] Hideaki Nanamiya,[1] Fujio Kawamura,[1,2] Tsuneyoshi Kuroiwa[1,2]†**

Chloroplast division involves plastid-dividing, dynamin, and FtsZ (PDF) rings. We isolated intact supertwisted (or spiral) and circular PDF machineries from chloroplasts of the red alga *Cyanidioschyzon merolae*. After individual intact PDF machineries were stretched to four times their original lengths with optical tweezers, they spontaneously returned to their original sizes. Dynamin-released PDF machineries did not retain the spiral structure and could not be stretched. Thus, dynamin may generate the motive force for contraction by filament sliding in dividing chloroplasts, in addition to pinching-off the membranes.

All life depends on photosynthesis by chloroplasts in plants for food and oxygen. Chloroplasts arose from an endosymbiotic cyanobacterial ancestor and have their own genomes that are maintained by division (*1*). Electron-dense rings, designated the outer and inner plastid-dividing (PD) rings, are found on the cytosolic and stromal faces of the membranes at the equator of dividing chloroplasts and are thought to be ubiquitous throughout the plant kingdom (*2*). The outer PD ring is composed of a bundle of fine filaments 5 to 7 nm in diameter and is most likely to be associated with the generation of the constriction force through sliding of the filaments (*2*, *3*). In addition, two types of guanosine triphosphatases (GTPases), FtsZ and dynamin, are thought to participate in chloroplast division. FtsZ is a nuclear-encoded homolog of a key bacterial division protein (*4*) and forms a ring on the stromal side at the equator (*5*), whereas dynamin is a eukaryote-specific membrane fission protein (*6*–*8*) and forms a ring at the cytosolic side alongside the PD ring (*9*, *10*). Chloroplast division is thought to be controlled by a PDF

[1]Laboratory of Cell Biology, Department of Life Science, College of Science, [2]Research Information Center for Extremophile, Rikkyo (St. Paul's) University, Toshima, Tokyo 171-8501, Japan.

*Present address: Department of Integrated Biosciences, Graduate School of Frontier Sciences, University of Tokyo 277-8562, Japan.

†To whom correspondence should be addressed. E-mail: tsune@rikkyo.ne.jp

# Supporting Online Material for

## Temporal and Spatial Enumeration Processes in the Primate Parietal Cortex

Andreas Nieder,* Ilka Diester, Oana Tudusciuc

*To whom correspondence should be addressed. E-mail: andreas.nieder@uni-tuebingen.de

Published 8 September 2006, *Science* **313**, 1431 (2006)
DOI: 10.1126/science.1130308

**This PDF file includes:**

# Supplementary Online Material

## Temporal and Spatial Enumeration Processes in the Primate Parietal Cortex

Andreas Nieder*, Ilka Diester, Oana Tudusciuc

*Primate NeuroCognition Laboratory, Hertie-Institute for Clinical Brain Research, Dept. of Cognitive Neurology, University of Tübingen, Otfried-Müller-Str. 27, 72076 Tübingen, Germany*

* To whom correspondence should be addressed: E-mail: andreas.nieder@uni-tuebingen.de

## Methods

***Stimuli.*** The items were black dots (diameter range 0.5 to 1.1 deg of visual angle) displayed on a gray background (diameter: 6 deg of visual angle). Successive dots (separated by short pauses during which only the gray background was visible) in the sequential protocol were presented in the center of the display, whereas the multiple dots in the simultaneous protocol were randomly arranged (see **Fig. 1a,b**). To prevent the monkeys from memorizing the visual patterns of the displays, each quantity was tested with 100 different images per session and the sample and test displays that appeared on every trial were never identical. All four quantities of items were used in each session and all displays were newly generated for each session by pseudo-randomly shuffling relevant item features (e.g., position and size in the multiple-item displays). Both the simultaneous and the sequential protocol were applied in each session with one standard and one control condition per protocol and appeared in random order with equal probability ($p = 0.25$). Non-numerical spatial and temporal cues were controlled across different quantities (**Table 1** and **Fig S1**).

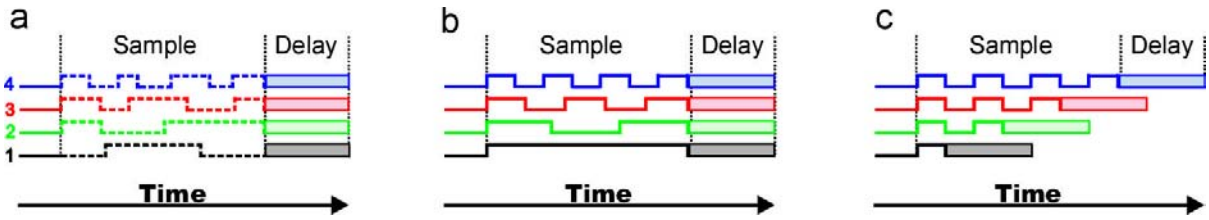


**Fig. S1:** Stimulus types for the sequential protocol followed by a constant delay period. (**a**) In the 'standard protocol', the duration of individual items and pauses in the sample period was pseudo-randomized from trial to trial (dotted lines in the stimulation illustration represent an example presentation layout) within a sample period of constant duration across numerosities. (**b**) In the 'equal sample duration' protocol, individual items and pauses had a constant duration for any given numerosity to match the constant duration of the entire sample period. (**c**) The duration of the items and pauses was equal across numerosities in the 'equal item/pause duration' protocol. Here, the duration of the sample period grew in proportion with the number of items. Monkeys had to match sequentially presented numerosities to numerosity in multiple-item displays.

***Behavioral protocol.*** A trial started when the monkey grasped a lever and fixated a central fixation target. After a 500 ms pure fixation period, the sample display period started, which lasted 800 ms in the simultaneous protocol. The sample period in the sequential protocol lasted 2500 ms; in few sessions the sample duration was extended to 3500 ms to further increase temporal variation. A constant 1000 ms memory delay followed. Next, a test

display appeared (always a multiple-dot display), which in 50 % of the cases was a match showing the same number of items as the sample period (match-trials). In the other 50 % of the cases (non-match trials) the first test display after the delay period was a non-match (it contained – with equal probability - either more or less items in the multiple-dot display, except for trials with sample numerosity "one") followed by a second test display which always was a match. If a match appeared, monkeys released the lever to receive a fluid reward. If a non-match was shown, they held the lever until the second test display appeared (which in these trials was always a match) requiring a lever release for a reward. Thus, the monkeys made the actual decision whether to release or maintain the lever during the presentation of the first test display (see **Fig. 1a,b**). Trials were randomized and balanced across all relevant features (e.g., match vs. non-match, sequential versus simultaneous, etc). **Fig. S2** shows the detailed behavioral performance functions of both monkeys in the sequential and the simultaneous protocol. Monkeys had to keep their gaze within 1.75 degree of the fixation point during sample presentation and the memory delay (monitored with an infrared eye tracking system).

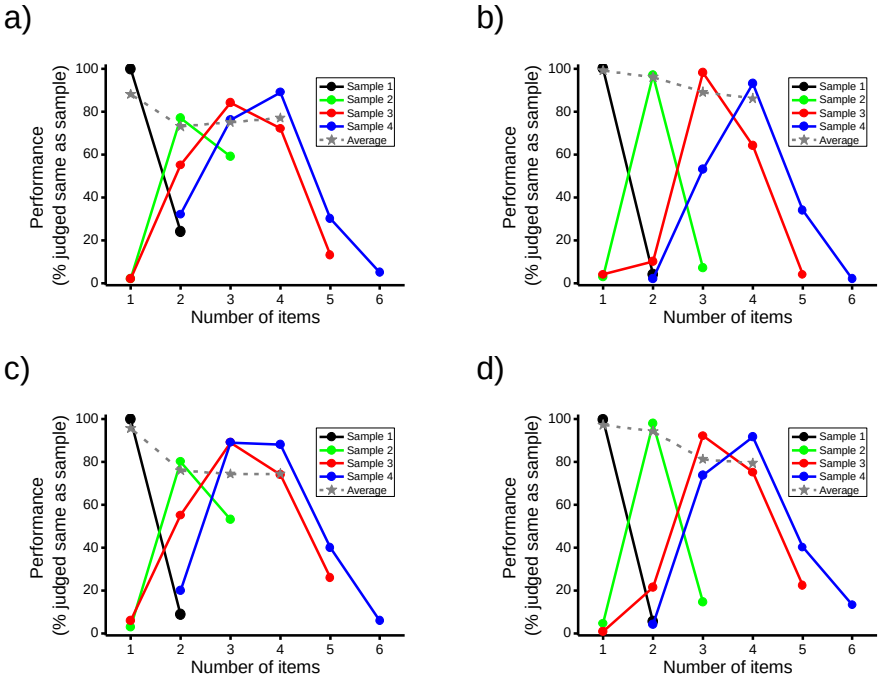


**Fig. S2:** Behavioral performance curves of monkey W (**a,b**) and monkey R (**c,d**) to the sequential (**a,c**) and simultaneous (**b,d**) stimulus protocols. The functions indicate the probability that a monkey judged displays in the test period as containing the same number of items as the sample numerosity. The center data point of each colored function indicates the correct performance in the match trials (where the first test display showed the same numerosity as had been cued in the sample period) for the four sample numerosities (see figure legend). The data points to the left and the right of the center indicate performance in the non-match trials (i.e., where the first test display showed a smaller or larger number of items); for the non-match numerosities the percentage of errors for the respective non-match numerosity is plotted. The red curve in **a)**, for example, represents all trials with 'three' as sample numerosity. The monkey judged correctly in 84 % of the presentations numerosity 'three' (center of the function) in the first test display as matching the sample numerosity (namely 'three'). When the non-match numerosity 'two' and 'one' appeared in the first test display, the monkey released the lever to indicate a numerical match in 55 % and 2 % of the trials, respectively, thus causing errors. Similarly, the monkey released the lever to the non-match numerosity 'four' and 'five' in the first test display to indicate a numerical match in 72 % and 13 % of the trials, respectively, thus causing again errors. The functions illustrate the numerical distance effect, i.e., it is more difficult for the monkey to discriminate close numerosities (3 versus 2 and 3 versus 4, in this example) than numerosities that are remote from each other (3 versus 1 and 3 versus 5).

***Training procedure.*** Both monkeys were first trained on the simultaneous protocol until they discriminated multiple-dot patterns reliably according to the number of items. Subsequently, they were gradually trained to enumerate sequential items throughout the course of several weeks. Monkeys could not be expected to immediately understand the logic of the sequential protocol because it had a completely different temporal design. We thus did not incorporate any transfer tests from simultaneous to sequential numerosity presentation.
Initially, the monkeys learned to discriminate only sequential numerosity 2 versus 4 (i.e., 4 was the non-match for sample 2, and 2 was the non-match for sample 4). To test whether they would grasp the concept of sequential numerosity after this basic training with 2 versus 4 sequential items, we tested the monkeys in transfer tests. Throughout the ongoing reinforced 2 versus 4 discrimination, we occasionally ($p = 0.1$) inserted transfer trials showing three consecutive items in the sample period. Non-match numerosities for transfer numerosity 3 were 2 and 4. Even though they were not reinforced for any particular response to sequential numerosity 3 (i.e., rewarded at chance), they discriminated sequential numerosity 3 from 2 and 4 with an accuracy comparable to that for the baseline discrimination for 2 and 4 (see **Fig. 1c,d**). After that, the entire range of sequential numerosities from 1 to 4 was introduced and correct responses were reinforced. Finally, the simultaneous and sequential protocols were mixed within a session. Recordings started after the animals performed both the sequential and simultaneous protocols and fixated reliably.

***Recording method.*** Recordings were made from one left and one right hemisphere in the depth of the intraparietal sulcus (IPS) of two rhesus monkeys (*Macaca mulatta*) in accordance with the guidelines for animal experimentation approved by the Regierungspräsidium Tübingen, Germany. This area was chosen because it contains the highest proportion of visual numerosity selective neurons (*23*) and is specifically activated by quantity information in humans (*17,19,21*). Arrays of four to eight tungsten microelectrodes (1 – 2 MOhm impedance) were inserted using a grid with 1-mm spacing. Recordings from the IPS were exclusively done at depths ranging from 9 mm to 13 mm below the cortical surface. Electrodes were advanced roughly perpendicular to the cortical surface passing through the lateral or medial bank. Recordings were localized using stereotaxic reconstructions from magnetic resonance images. The Horsley-Clark coordinates of the IPS recordings ranged from 2 mm posterior to 3 mm anterior (see "Visual direction selectivity of neurons"). Both monkeys are still engaged in quantity discrimination studies. Neurons were selected at random; no attempt was made to search for any task-related activity. Separation of single-unit waveforms was performed off-line applying mainly principal component analysis.

***Data analysis.*** In the simultaneous condition, sample activity was derived from an 800 ms interval after stimulus onset shifted by a cell's individual response latency. In the sequential condition, the spike rate to each individual item in the sample period was measured after deriving the precise onset and duration of any given item on a trial-by-trial basis (for the standard sequential protocol, single items' onsets and durations were pseudo-randomly chosen by the computer program prior to each single presentation). Again, the analysis window for every item was shifted by the neurons' response latency. To measure neuronal response latency, we generated average spike density histograms (at 1 ms resolution, smoothed by a sliding window, kernel bin width: 10 ms) for a neuron's responses to all sample stimuli. Discharges following sample onset were compared to spike rates in a 200 ms interval preceding sample onset. Response latency was defined by the first time bin that reached a value higher or lower than any value before sample onset. A default latency of 100 ms was

used if no measure based on these criteria could be derived. For the delay period, activity was summed in a 800 ms interval starting 200 ms after delay onset.
To determine numerosity-selectivity for the sample period in the sequential and simultaneous protocol separately, a two-factorial analysis of variance (ANOVA) was calculated with numerosity (one to four) and stimulation condition (standard or control) as factors. In the delay period, a two-factorial ANOVA was computed with numerosity (one to four) and stimulus protocol (sequential or simultaneous) as factors. All ANOVAs were calculated with the square-root transformed spike rates values to render spike rate distributions normal and to equalize the population variances (*1*). ANOVAs were calculated separately for sequences of two, three and four items. A neuron was judged to be numerosity selective in the sequential protocol if the preferred numerosity was the same in all separate analyses for two, three and four items in a sequence. Numerosity-selectivity in the simultaneous protocol was derived during the 800 ms sample period (**Fig. S3**).
To derive averaged numerosity-filter functions, the tuning functions of individual neurons were normalized by setting the maximum activity to the most preferred quantity as 100 % and the activity to the least preferred quantity as 0 %. Pooling the resulting normalized tuning curves resulted in averaged numerosity-filter functions.

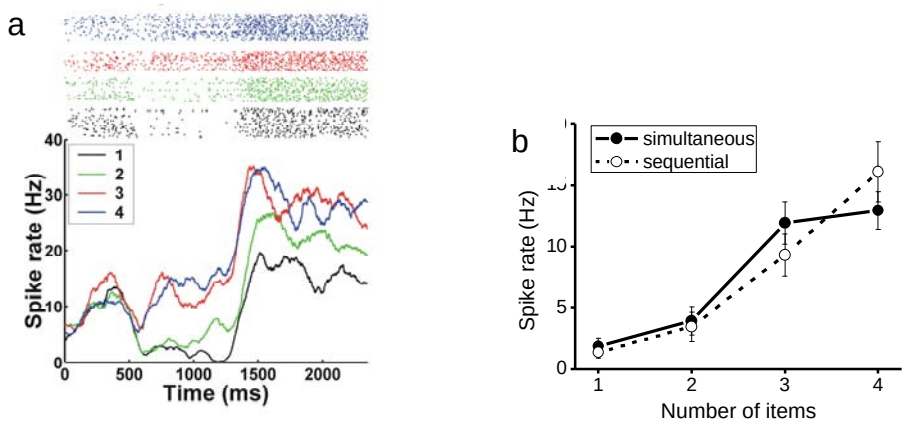


**Fig. S3**: Responses of the neuron shown in Fig. 2f-h to the simultaneous protocol. (**a**) Dot-raster histogram and spike-density histogram derived from the discharges to multiple-item displays. (Sample onset at 500 ms, delay onset at 1300 ms). This neuron belonged to one of the two cells tuned to the same numerosity 'four' in both the simultaneous and the sequential protocol as indicated by the tuning functions (**b**). This neuron was also selective during the delay period.

***Multiple regression analysis.*** To statistically assess whether temporal parameters influenced the activity of numerosity-selective neurons to their preferred sequential item, we performed a multiple linear regression analysis using the following regression model:

$$y = ß_0 + ß_1*x_1 + ß_2*x_2 + ß_3*x_3$$

where $y$ is the discharge rate to the preferred sequential item, $x_1$ is the duration of the preferred item in a sequence, $x_2$ is the duration of the pause preceding the preferred item, and $x_3$ is the duration of the previous-to-preferred item. (For neurons selective to the first item, a simple linear regression was applied). Furthermore, $ß_0$ is the intercept, and $ß_{1\text{-}3}$ are the corresponding regression coefficients.
We calculated the probability that at least one of the coefficients equalled zero by an F-statistic. Furthermore, we got the significance values for each parameter by a t-test. If at least

one of the tests was significant with $p < 0.01$, the neuronal activity was accepted as reflecting non-numerical temporal factors and the cell was excluded from the pool of numerosity-selective neurons. Correlation coefficients for discharges to the preferred sequential item as a function of the above temporal parameters are displayed in **Fig. S4**.

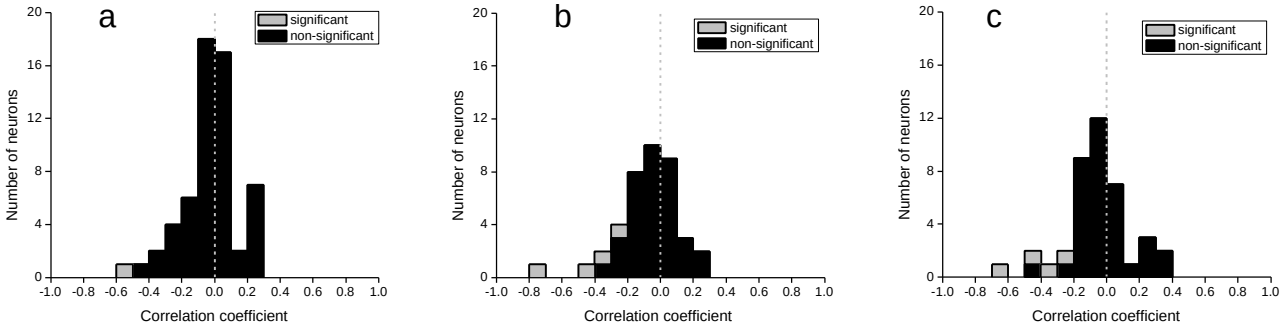


**Fig. S4**: Correlation coefficients derived from multiple linear regression analysis to test the influence of temporal factors on the discharge of neurons selective for sequential numerosity. Frequency histograms of correlations coefficients for (a) the duration of the preferred item in a sequence, *(b)* the duration of the pause preceding the preferred item, and *(c)* the duration of the previous-to-preferred item are plotted. Few of the neurons discharged significantly as a function of temporal parameters.

With the same regression model, we tested the influence of temporal parameters on the discharges to the preferred pause in between sequential items. In this case, however, $y$ is the discharge rate to the preferred pause in between sequential items, $x_1$ is the duration of the preferred pause in a sequence, $x_2$ is the duration of the item preceding the preferred pause, and $x_3$ is the duration of the previous-to-preferred pause. Correlation coefficients for discharges to the preferred sequential pause as a function of the above temporal parameters are displayed in **Fig. S5**.

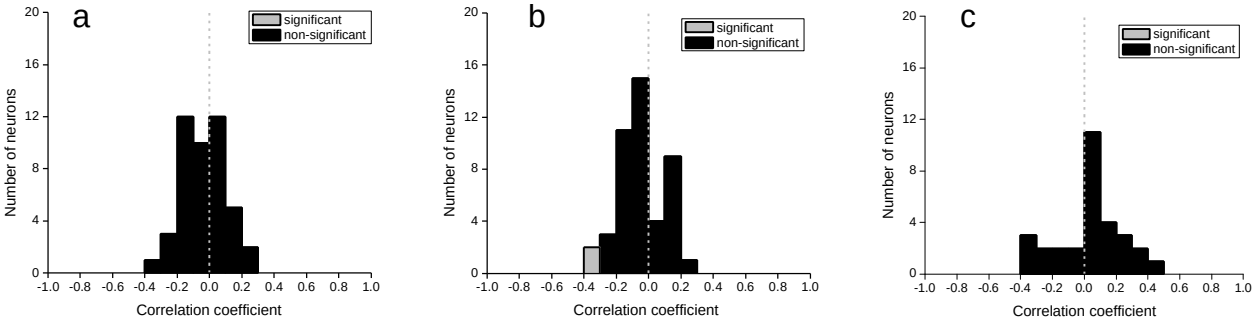


**Fig. S5**: Correlation coefficients derived from multiple linear regression analysis to test the influence of temporal factors on the discharge of neurons selective for pauses between sequentially displayed items. Frequency histograms of correlations coefficients for (**a**) the duration of the preferred pause in a sequence, *(***b***)* the duration of the item preceding the preferred pause, and *(***c***)* the duration of the previous-to-preferred pause are plotted. Only two of the neurons discharged significantly as a function of the duration of the item preceding the preferred pause.

***Test for visual motion direction selectivity.*** Many neurons were additionally tested with flow field stimuli to investigate the location of numerosity-selective recordings sites relative to ventral intraparietal area (VIP), an area containing a high proportion of visual direction selective cells (*2*). The stimuli consisted of white randomly distributed dots (0.06 deg. of vis. angle, 10 % density) coherently moving on a circular black background (23 deg. of vis. angle) in one of 6 possible directions (up, down, left, right at a speed of 5.4 deg. of vis. angle; approaching and receding at a speed of 9 deg. of vis. angle). The flow field stimuli were presented for 500 ms at a 60 Hz refresh rate. The animals were rewarded for passively viewing the stimuli while maintaining gaze fixation within 1.5 degree of the fixation point. Blocks of flow field stimulus presentation were randomly interleaved throughout the ongoing numerosity discrimination. Neurons were included in the analysis if at least six repetitions of each motion direction could be presented. Neuronal responses were derived in 500 ms windows (shifted by the neurons' individual latencies relative to motion onset, or by a default 80 ms for those neurons where latency could not be determined) and statistically evaluated by a Kruskal-Wallis test at criterion of $p < 0.05$.

Sufficient stimulus repetitions could be presented at 114 recording sites in the fundus of the IPS (see "Recording method" for anatomical coordinates). At 63 of these sites, one or more single-units were found (based on spike sorting) that were significantly tuned to motion direction (**Fig. S6**); thus 55 % of our recording sites exhibited visual motion direction selectivity, arguing for VIP-recordings. Note that our proportion of motion direction selective neurons constitutes a conservative estimate based on the relatively few numbers of repetitions and the restricted range of motion directions and speeds (which was due to the time constraints placed by the actual numerosity task). Note also that our recordings were completely unbiased with respect to the neurons' response properties; every neuron that could be well isolated was incorporated into this analysis. Interestingly, we often recorded pairs or triplets of neurons at the same electrode that responded differently to the motion patterns. In 33 recording sites where at least two units could be isolated, 9 of them (27%) had all their units selective for motion direction (but rarely to the same direction), the other 24 (72 %) had at least one unit which was not tuned to any direction (**Fig. S7**).

In addition to this quantitative evaluation of motion direction selectivity, we often tested qualitatively for responses to tactile stimulation by touching different parts of the monkeys' heads; we frequently detected correlated discharges when touching head parts (primarily contralateral to the recording site). Since VIP neurons are also characterized by somatosensory responses (*3*), this is another indication that we recorded in area VIP.

We managed to test 75 cells that turned out to be tuned to numerosity (in any trial period) for visual direction selectivity. Roughly half of them (38/75 or 51 %) were both motion direction selective and numerosity selective. This argues for partly overlapping neuronal networks engaged in motion direction and numerical information processing.

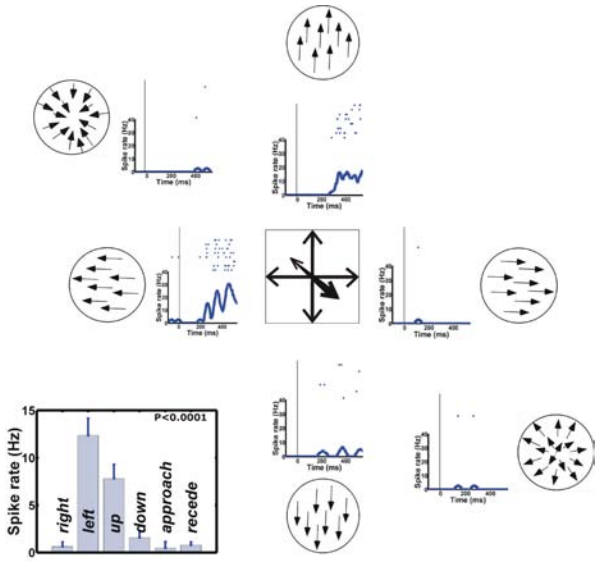


**Fig. S6:** Neuron in the fundus of the IPS showing a high degree of visual direction selectivity to flow field stimuli with leftward motion. The center panel illustrates the motion direction of the dot patterns. The neuronal responses for eight repetitions of each stimulus (see arrow drawings) are shown as dot-raster histograms (top panels) and averaged spike density histograms (bottom panels). Time 0 ms (vertical line) indicates motion onset; each stimulus was shown for 500 ms. The column plot in the left lower corner shows the mean discharge (error bars represent SEM) to the six directions; the p-value of the Kruskal-Wallis test indicates highly significant selectivity. This neuron was not numerosity-selective.

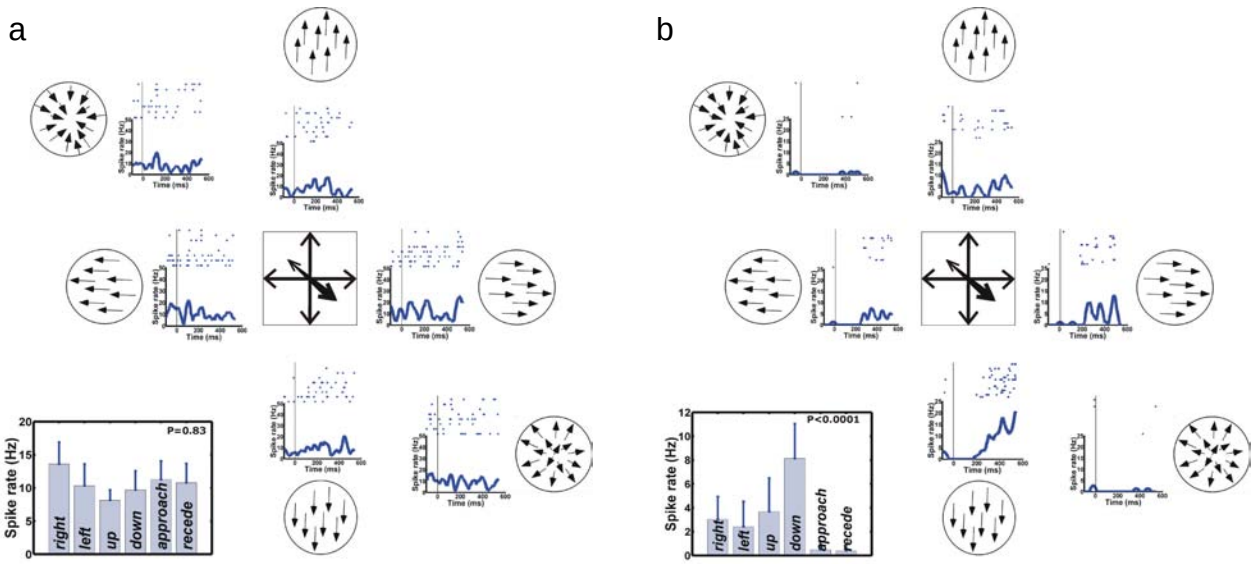


**Fig. S7:** Two neurons recorded simultaneously at the same electrode (layout as in **Fig. S6**). **a)** The single unit is the same as in **Fig. 2f**, which was selectively tuned to sample numerosity 'four' in the sequential protocol. This neuron was not tuned to visual motion direction. **b)** Interestingly, an immediately adjacent neuron recorded at the same location exhibited strong directionality (to downward motion), but no tuning to numerosity.

---

[1] Sachs, L. (1992) *Angewandte Statistik*. 7. ed., Springer Verlag.

[2] Colby C.L., Duhamel J.R. & Goldberg M.E. Ventral intraparietal area of the macaque – anatomical location and visual response properties. *J. Neurophysiol.* **69**, 902-914 (1993).

[3] Duhamel J.R., Colby C.L., Goldberg M.E. Ventral intraparietal area of the macaque: congruent visual and somatic response properties. *J. Neurophysiol.* **79**, 126-36 (1998).